# Supplemental Information

# Design, synthesis and evaluation of liver-targeting fluorescent probe for detecting mercury ion

**Wei Hu [a], Jianyi Wang*[b]**

[a] *State Key Laboratory for Conservation and Utilization of Subtropical Agro-Bioresources, Guangxi University, Nanning 530004, China*

[b] *Medical College, Guangxi University, Nanning 530004, China*

* Corresponding author: jianyi Wang, email: jianyiwang@gxu.edu.cn

## Figures and captions

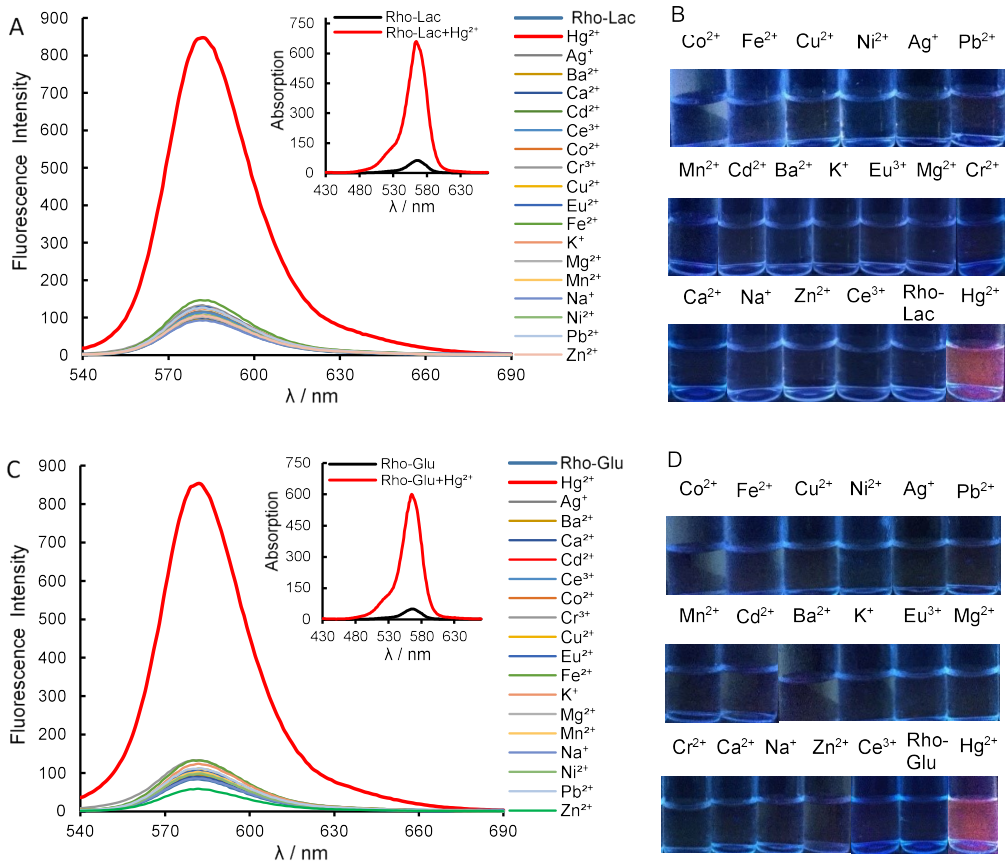


**Fig.S1** Fluorescence response of probes toward different metal ions. The $Hg^{2+}$ aqueous solution of 50 μM was added into the probes solution of 5 μM (10 mM stock solution dissolved in DMSO, then diluted using water). Fluorescence determination of Rho-Lac (A) and Rho-Glu (C) via fluorescence spectrophotometer. Fluorescence response of Rho-Lac (B) and Rho-Glu (D) using Ultra-Violet irradiation.

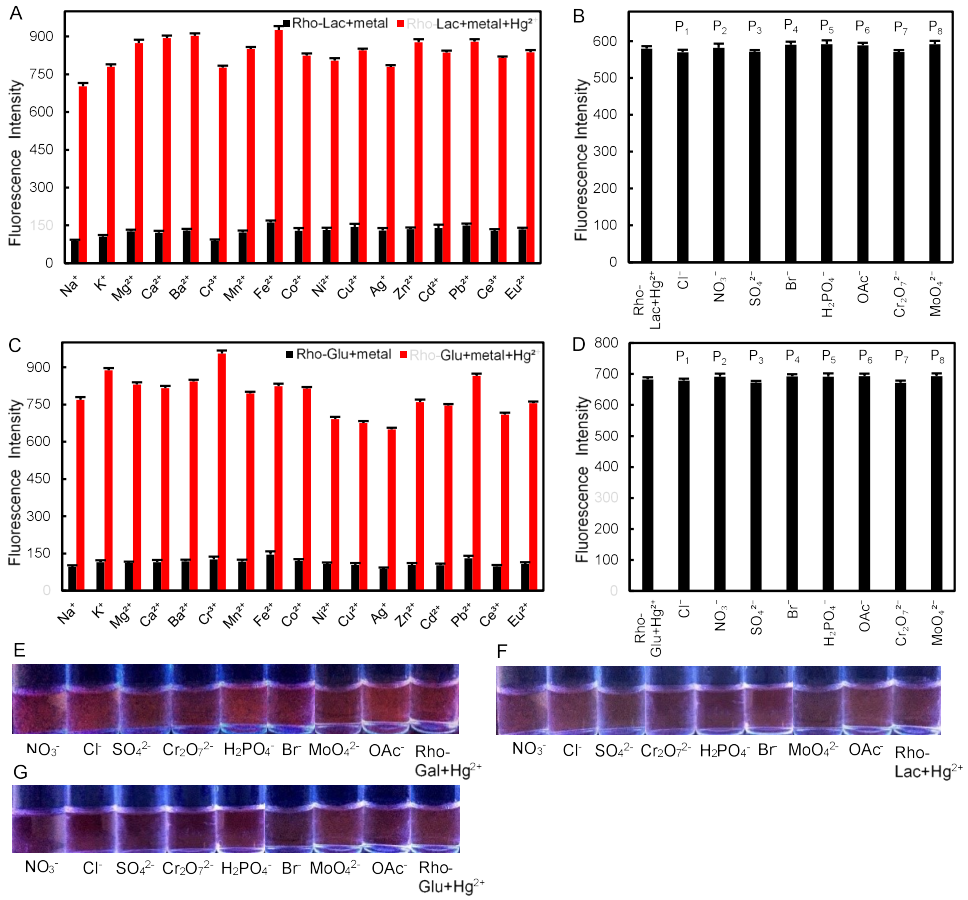


**Fig. S2** Fluorescent signal alterations of probes to $Hg^{2+}$ with other ions. Metal ions competition of Rho-Lac (A) and Rho-Glu (C). Data was analyzed using a two-way RMANOVA test (different metal ions × addition of $Hg^{2+}$ interaction). Rho-Lac, $F(1, 136) = 249099.5$ and $P < 0.0001$, for whether to add $Hg^{2+}$; Rho-Glu, $F(1, 136) = 277322$ and $P < 0.0001$, for whether to add $Hg^{2+}$. Anions interference of Rho-Lac (B) and Rho-Glu (D). Data was analyzed using a one-way ANOVA test. $P > 0.05$, compared with Rho-Lac+$Hg^{2+}$ ($P_1$=0.061252, $P_2$=0.673622, $P_3$= 0.062108, $P_4$=0.062898, $P_5$=0.058265, $P_6$= 0.05968, $P_7$= 0.057582, $P_8$=0.050567); $P > 0.05$, compared with Rho-Glu+$Hg^{2+}$ ($P_1$=0.49376, $P_2$=0.173098, $P_3$=0.052019, $P_4$=0.05616, $P_5$= 0.190145, $P_6$=0.065849, $P_7$=0.052146, $P_8$= 0.09182). Anions interference for Rho-Gal (E), Rho-Lac (F) and Rho-Glu (G) using Ultra-Violet irradiation.

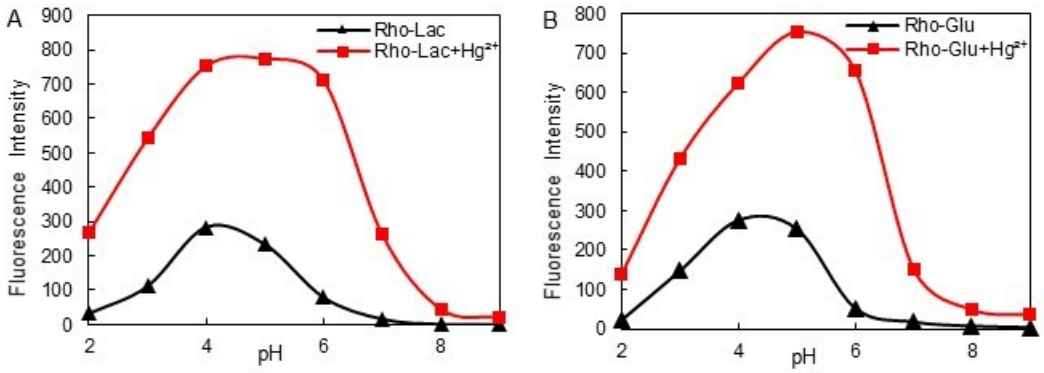


**Fig. S3** Fluorescence alternations of Rho-Lac (A) and Rho-Glu (B) in different pH. The 5 μM probes solution and 10 μM $Hg^{2+}$ solution were prepared with different pH value using HAc-NaOAc buffer at pH value of 2, 3, 4, 5, 6, 7, 8, and 9 respectively.

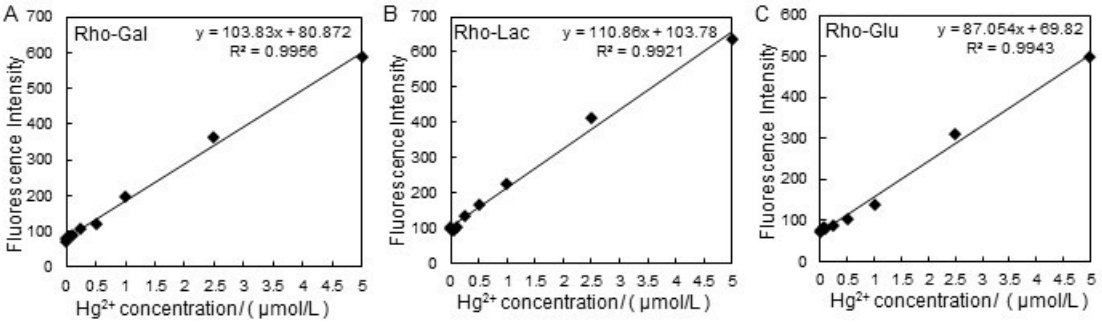


**Fig. S4** Linearity between $Hg^{2+}$ concentration and fluorescence intensity. The 5 μM Rho-Gal(A), Rho-Lac (B) and Rho-Glu (C) probes solution were added with $Hg^{2+}$ solution of 0.01, 0.05, 0.1, 0.25, 0.5, 1.0, 2.5, 5 μM respectively to detect the fluorescence response value.

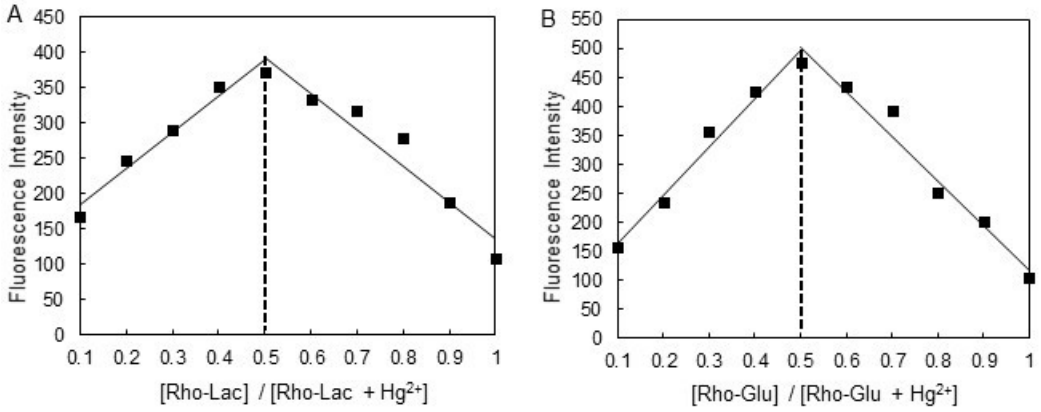


**Fig. S5** Job's plot of Rho-Lac (A) and Rho-Glu (B) probes-$Hg^{2+}$. The $Hg^{2+}$, probes solution (10 mM stock solution in DMSO) were prepared and diluted using water to keep the total concentration of probes and $Hg^{2+}$ solution at 10 μM.

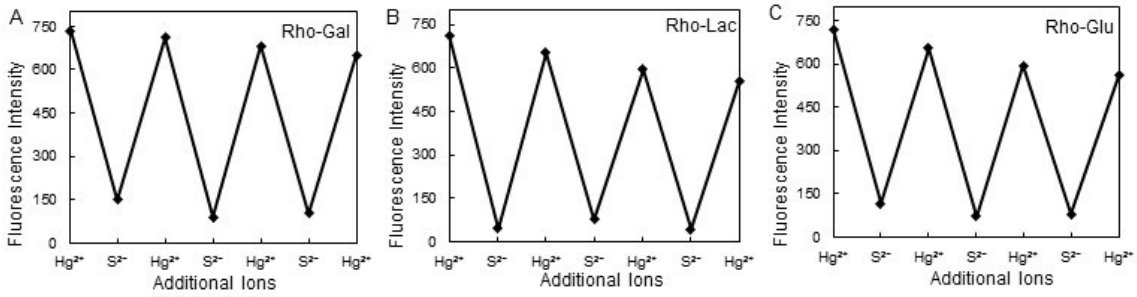


**Fig. S6** Fluorescent cycle changes of Rho-Gal (A), Rho-Lac (B) and Rho-Glu (C) to $Hg^{2+}$ with addition of $S^{2-}$. The probes stock solution of 10 mM were prepared with DMSO, then diluted to 5 μM using water. The $Hg^{2+}$ and $S^{2-}$ solution of 50 μM also was dissolved in water.

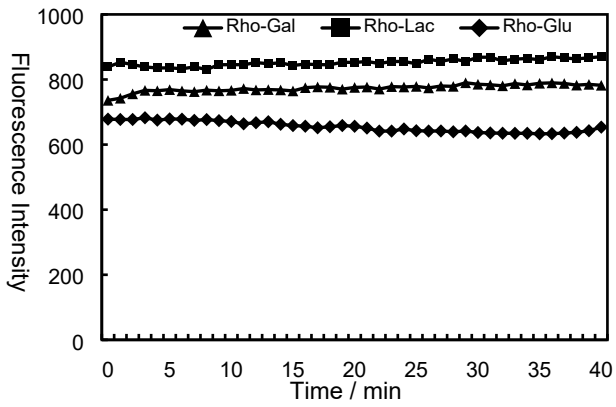


**Fig. S7** Fluorescence stability of probes toward $Hg^{2+}$. $Hg^{2+}$ solution with 50 μM was added into the 5 μM probes solution, and the fluorescence response was continuously detected at 1 min interval within 40 min.

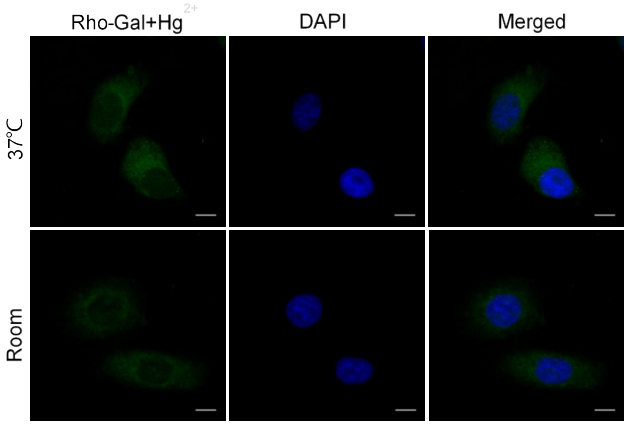


**Fig. S8** Fluorescence response of Rho-Gal to $Hg^{2+}$ in dead cells (scale bar 10 μm). Two copies of HepG2 cells fixed for 15 min were prepared. One was treated with 20 μM Rho-Gal solution at room temperature for 20 min, and incubated with 200 μM $Hg^{2+}$ solution at room temperature for 15 min, then stained with DAPI for 5 min. Another was incubated with 20 μM Rho-Gal solution at 37 ° C for 20 min, incubated with 200 μM $Hg^{2+}$ solution at 37 ° C for 15 min, and stained with DAPI for 5 min. Then the cellular fluorescence imaging was acquired.

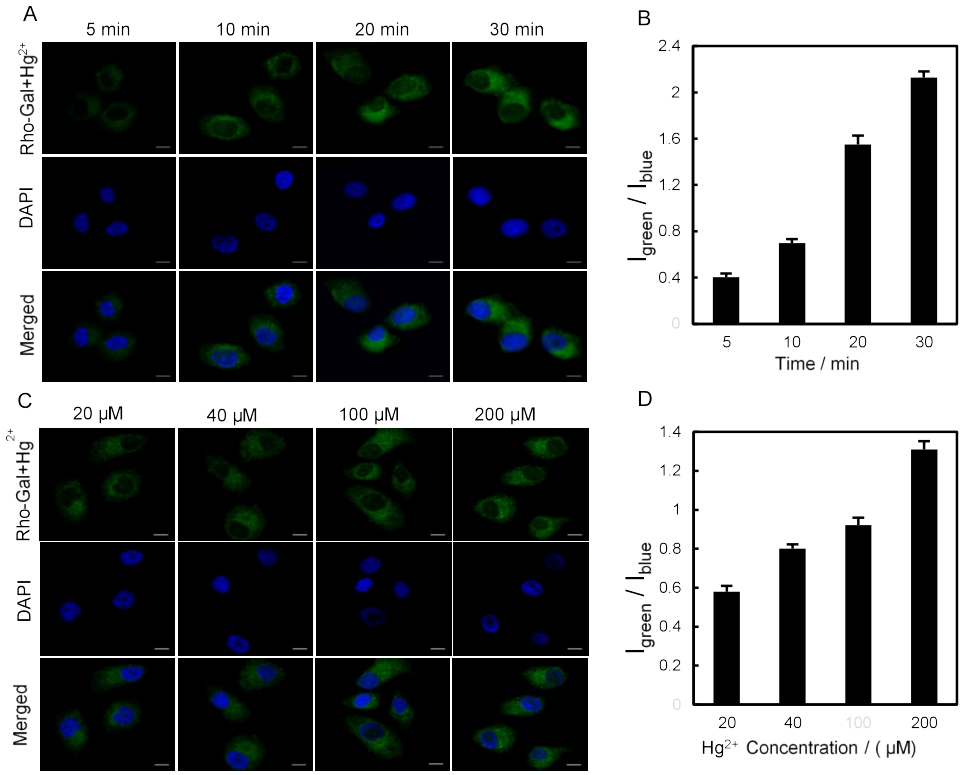


**Fig. S9** Intracellular fluorescence manners of Rho-Gal to $Hg^{2+}$. The scale bar is 10 μm. Igreen and Iblue is the fluorescence intensity of Rho-Gal+$Hg^{2+}$ and DAPI respectively. Cellular fluorescence imaging in quintuplicate was acquired and data was analyzed using a one-way ANOVA, $P< 0.0001$. (A) (B) Rho-Gal incubated with HepG2 cells for different time. HepG2 cells were incubated in incubator with 20 μM Rho-Gal solution dissolved in DMEM for 5, 10, 20 and 30 min, respectively, then incubated with 200 μM $Hg^{2+}$ solution dissolved in DMEM for 15 min, fixed for 15 min, and treated with DAPI for 5 min. Cellular fluorescence imaging in quintuplicate was acquired. (C) (D) Rho-Gal reacted with different concentration of $Hg^{2+}$ in HepG2 cells. HepG2 cells were incubated with 20 μM Rho-Gal dissolved in DMEM in incubator for 15 min, then incubated with $Hg^{2+}$ solution dissolved in DMEM with different concentration of 20, 40, 100 and 200 μM in incubator for 15 min, fixed for 15 min and treated with DAPI for 5 min.

## Characterization of compounds

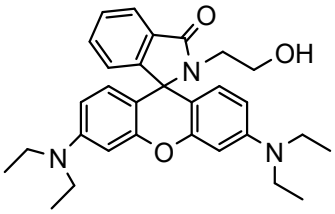


The compound was gray white solid, yield 35%. $^1$H NMR (600 MHz, $CDCl_3$) δ 7.92 (dd, $J$ = 5.6, 3.0 Hz, 1H), 7.46 (dd, $J$ = 5.6, 3.1 Hz, 2H), 7.09 (dd, $J$ = 5.2, 3.2 Hz, 1H), 6.51 (d, $J$ = 8.9 Hz, 2H), 6.40 (d, $J$ = 2.4 Hz, 2H), 6.31 (dd, $J$ = 8.9, 2.4 Hz, 2H), 3.51 – 3.47 (m, 2H), 3.36 (q, $J$ = 7.0 Hz, 8H), 3.32 – 3.29 (m, 2H), 1.19 (t, $J$ = 7.1 Hz,12H). $^{13}$C NMR (151 MHz, $CDCl_3$) δ 170.10, 153.92, 153.28, 148.90, 132.69,

130.45, 128.51, 128.14, 123.81, 122.90, 108.24, 104.80, 97.80, 65.87, 62.68, 62.66, 44.65, 44.37, 12.61.

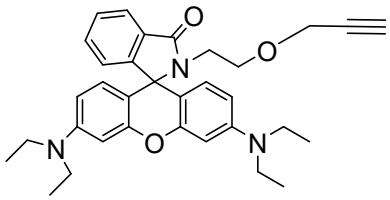

The compound was grey white solid, yield 86%. $^1$H NMR (600 MHz, $CDCl_3$) δ 7.94 – 7.90 (m, 1H), 7.46 – 7.43 (m, 2H), 7.12 – 7.07 (m, 1H), 6.46 (d, *J* = 8.9 Hz, 2H), 6.40 (d, *J* = 2.6 Hz, 2H), 6.29 (dd, *J* = 8.9, 2.6 Hz, 2H), 3.91 (d, *J* = 2.4 Hz, 2H), 3.37 (dq, *J* = 14.2, 7.1 Hz, 10H), 3.24 (t, *J* = 7.0 Hz, 2H), 2.30 (t, *J* = 2.4 Hz, 1H), 1.18 (t, *J* = 7.1 Hz, 12H).

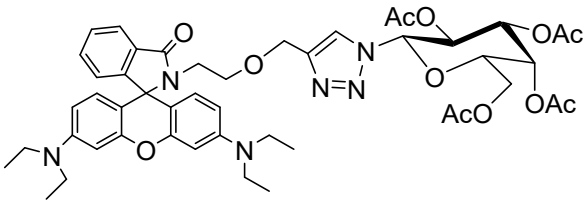

The compound was light red solid, yield 88%. $^1$H NMR (600 MHz, $CDCl_3$) δ 7.90 – 7.86 (m, 1H), 7.77 (s, 1H), 7.42 – 7.38 (m, 2H), 7.07 – 7.03 (m, 1H), 6.42 (dd, *J* = 8.9, 4.9 Hz, 2H), 6.36 (d, *J* = 2.4 Hz, 2H), 6.29 – 6.22 (m, 2H), 5.78 (d, *J* = 9.3 Hz, 1H), 5.56 – 5.50 (m, 2H), 5.21 (dd, *J* = 10.3, 3.3 Hz, 1H), 4.40 – 4.35 (m, 2H), 4.20 – 4.17 (m, 1H), 4.12 – 4.07 (m, 2H), 3.38 (t, *J* = 7.2 Hz, 2H), 3.31 (q, *J* = 7.0 Hz, 8H), 3.18 (dt, *J* = 9.4, 7.1 Hz, 2H), 2.21 (s, 3H), 2.01 (s, 3H), 1.98 (s, 3H), 1.83 (s, 3H), 1.14 (t, *J* = 7.0 Hz, 12H).

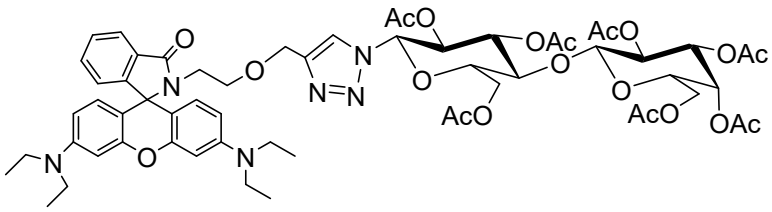

The compound was light red solid, yield 84%. $^1$H NMR (600 MHz, $CDCl_3$) δ 7.93 – 7.90 (m, 1H), 7.71 (s, 1H), 7.46 – 7.42 (m, 2H), 7.11 – 7.07 (m, 1H), 6.45 (dd, *J* = 8.8, 7.0 Hz, 2H), 6.39 (d, *J* = 1.7 Hz, 2H), 6.27 (dd, *J* = 8.9, 2.4 Hz, 2H), 5.78 (d, *J* = 8.8 Hz, 1H), 5.41 (ddd, *J* = 10.6, 9.4, 6.3 Hz, 3H), 5.15 (dd, *J* = 10.4, 7.9 Hz, 1H), 4.99 (dd, *J* = 10.4, 3.5 Hz, 1H), 4.54 (d, *J* = 7.9 Hz, 1H), 4.47 (dd, *J* = 12.1, 1.7 Hz, 1H), 4.38 (s, 2H), 4.14 (qd, *J* = 11.2, 6.6 Hz, 3H), 3.99 – 3.95 (m, 1H), 3.94 – 3.88 (m, 2H), 3.41 (t, *J* = 7.2 Hz, 2H), 3.35 (q, *J* = 7.0 Hz, 8H), 3.22 – 3.18 (m, 2H), 2.18 (s, 3H), 2.11 (s, 3H), 2.10 (s, 3H), 2.07 (s, 6H), 1.99 (s, 3H), 1.84 (s, 3H), 1.18 (td, *J* = 6.9, 1.0 Hz, 12H).

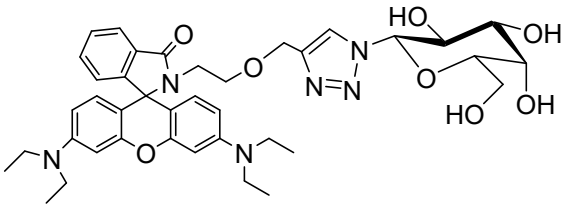

**Rho-Gal**, light red solid, yield 92%. $^{1}$H NMR (600 MHz, $CDCl_3$) δ 8.00 (s, 1H), 7.81 (d, *J* = 6.7 Hz, 1H), 7.38 – 7.32 (m, 2H), 7.00 (d, *J* = 6.6 Hz, 1H), 6.39 – 6.34 (m, 4H), 6.26 – 6.21 (m, 2H), 5.57 (d, *J* = 9.0 Hz, 1H), 4.33 (t, *J* = 9.1 Hz, 1H), 4.26 (s, 2H), 4.18 (s, 1H), 3.87 – 3.77 (m, 4H), 3.28 (dd, *J* = 13.7, 6.6 Hz, 10H), 3.07 (t, *J* = 6.2 Hz, 2H), 1.11 (t, *J* = 7.0 Hz, 12H). $^{13}$C NMR (151 MHz, $CD_3OD$) δ 168.85, 153.74, 153.35, 149.01, 144.74, 132.72, 130.54, 128.30, 128.09, 123.66, 122.26, 122.18, 108.21, 104.76, 97.66, 88.86, 78.54, 73.91, 70.05, 68.96, 66.90, 65.52, 63.26, 61.01, 43.99, 39.00, 11.51. HRMS: $[M+H]^+$ calculated for $C_{39}H_{49}N_6O_8$, m/z 729.36064, measured m/z 729.36157. mp 165.3-167.9.

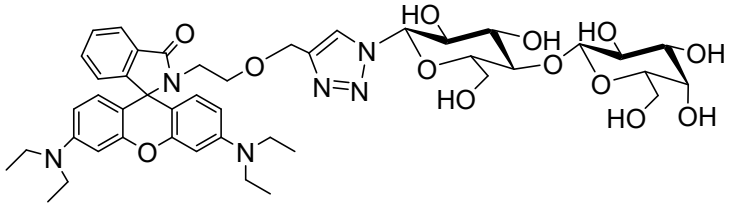

**Rho-Lac**, light red solid, yield 91%. $^{1}$H NMR (600 MHz, $CD_3OD$) δ 8.05 (s, 1H), 7.88 – 7.84 (m, 1H), 7.52 – 7.48 (m, 2H), 7.03 – 7.00 (m, 1H), 6.43 (s, 2H), 6.34 (d, *J* = 0.9 Hz, 4H), 5.61 (d, *J* = 9.2 Hz, 1H), 4.43 (d, *J* = 7.7 Hz, 1H), 4.29 (s, 2H), 3.95 (t, *J* = 9.1 Hz, 1H), 3.89 (d, *J* = 2.9 Hz, 2H), 3.84 (d, *J* = 3.2 Hz, 1H), 3.80 (td, *J* = 11.1, 8.6 Hz, 2H), 3.73 (ddd, *J* = 12.8, 9.1, 3.1 Hz, 3H), 3.63 (dd, *J* = 7.5, 4.7 Hz, 1H), 3.59 (dd, *J* = 9.6, 7.8 Hz, 1H), 3.52 (dd, *J* = 9.7, 3.3 Hz, 1H), 3.36 (q, *J* = 7.0 Hz, 8H), 3.12 (t, *J* = 6.6 Hz, 2H), 1.14 (t, *J* = 7.0 Hz, 12H). $^{13}$C NMR (151 MHz, $CD_3OD$) δ 168.86, 153.74, 153.35, 149.02, 144.69, 132.73, 130.53 , 128.29 , 128.11 , 123.66, 122.63, 122.18, 108.21, 104.74, 103.71, 97.65, 87.94, 78.26, 78.15, 75.75, 75.41, 73.43, 72.28, 71.16, 68.93, 66.93, 65.53, 63.25, 61.15, 60.14, 43.99, 38.99 , 11.51. HRMS: $[M+H]^+$ calculated for $C_{45}H_{59}N_6O_{13}$, m/z 891.41346, measured m/z 891.41516. mp 176.5-179.6.

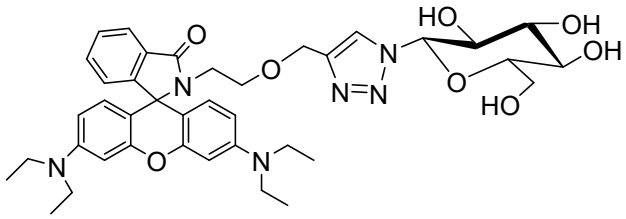

**Rho-Glu**, light red solid, yield 83%. $^{1}$H NMR (600 MHz, $CD_3OD$) δ 8.06 (s, 1H), 7.87 (dt, *J* = 5.9, 2.5 Hz, 1H), 7.54 – 7.49 (m, 2H), 7.04 – 7.02 (m, 1H), 6.45 (s, 2H), 6.39 – 6.34 (m, 4H), 5.59 (d, *J* = 9.2 Hz, 1H), 4.30 (s, 2H), 3.92 – 3.87 (m, 2H), 3.72 (dd, *J* = 12.2, 5.3 Hz, 1H), 3.61 – 3.55 (m, 2H), 3.55 – 3.50 (m, 1H), 3.38 (q, *J* = 7.0 Hz, 8H), 3.34 – 3.32 (m, 2H), 3.13 (t, *J* = 6.6 Hz, 2H), 1.16 (t, *J* = 7.0 Hz, 12H). $^{13}$C

NMR (151 MHz, $CD_3OD$) δ 168.85, 153.74, 153.35, 149.02, 144.65, 132.73, 130.54, 128.29 128.10, 123.66, 122.64, 122.17 108.21, 104.75, 97.65, 88.21, 79.73, 77.06, 72.65, 69.49, 66.92, 65.52, 63.25, 61.01, 43.99, 38.98, 11.51. HRMS: $[M+H]^+$ calculated for $C_{39}H_{49}N_6O_8$, m/z 729.36064, measured m/z 729.36194. mp 164.6-167.5.

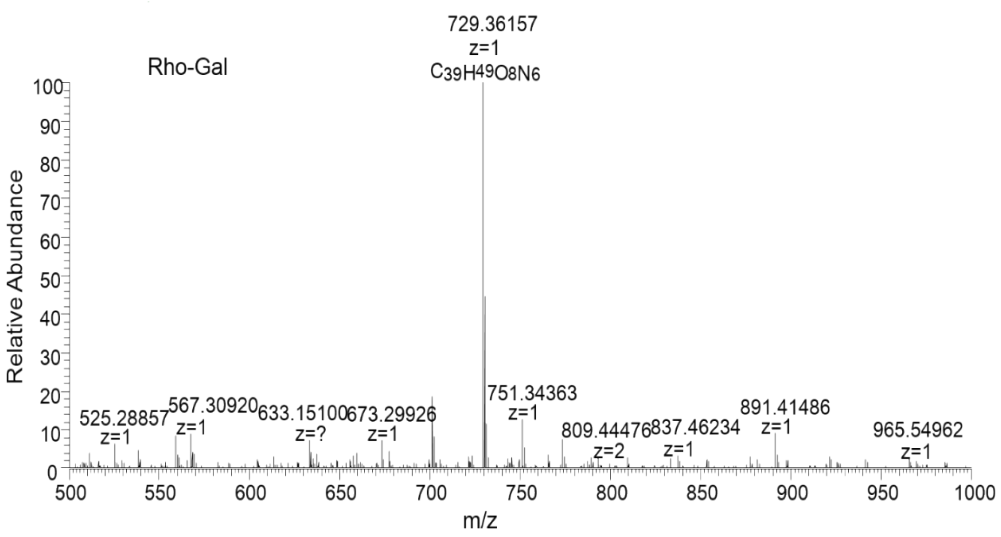


**Fig. S10** Mass spectrum of Rho-Gal

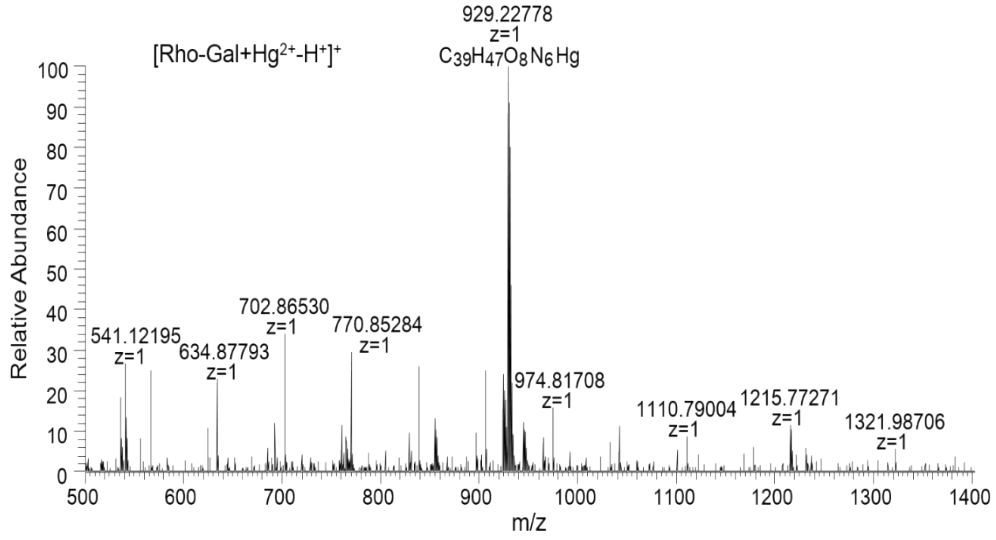


**Fig. S11** Mass spectrum of Rho-Gal-$Hg^{2+}$ complex

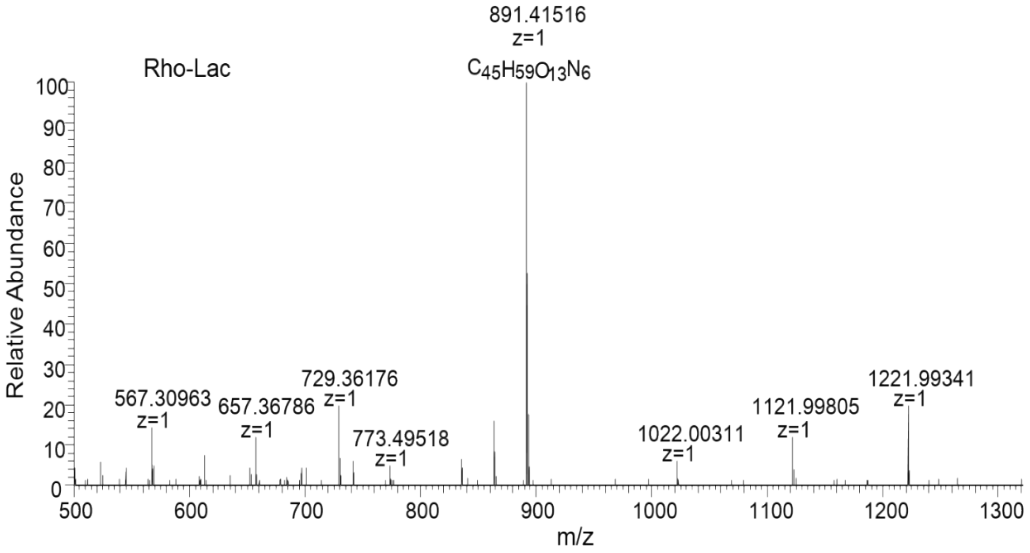


**Fig. S12** Mass spectrum of Rho-Lac

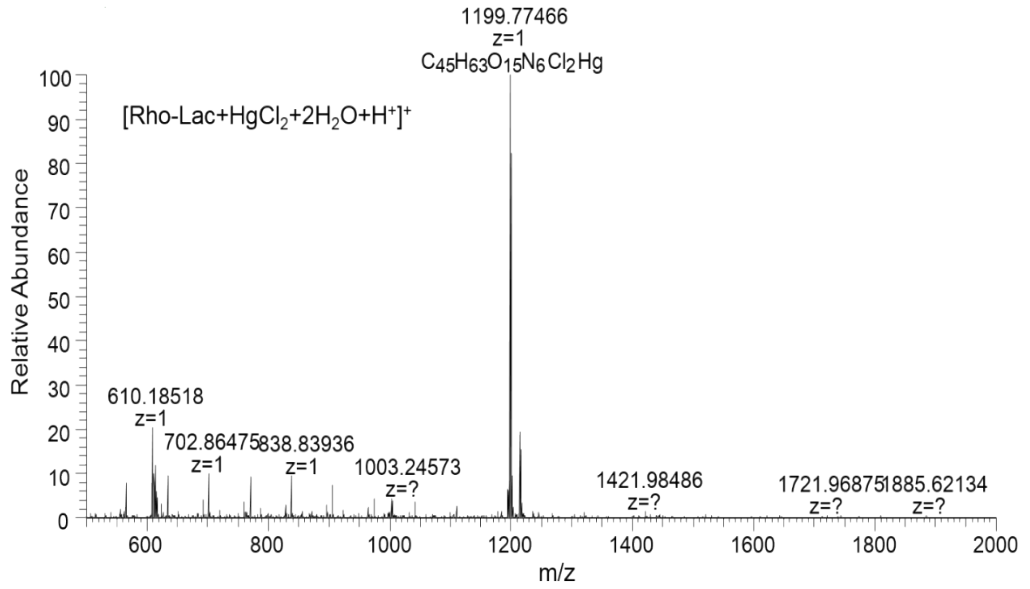


**Fig. S13** Mass spectrum of Rho-Lac-$Hg^{2+}$ complex

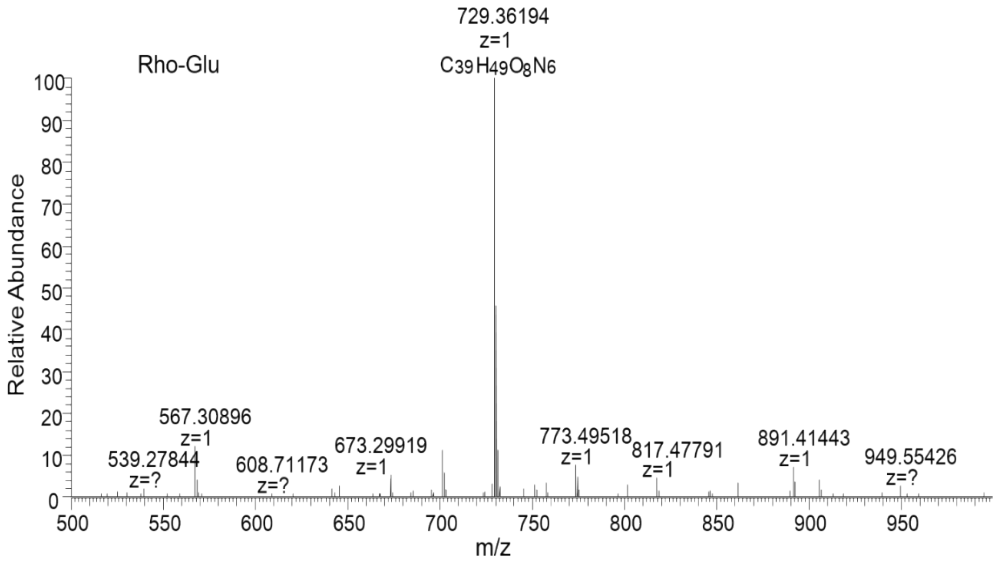


**Fig. S14** Mass spectrum of Rho-Glu

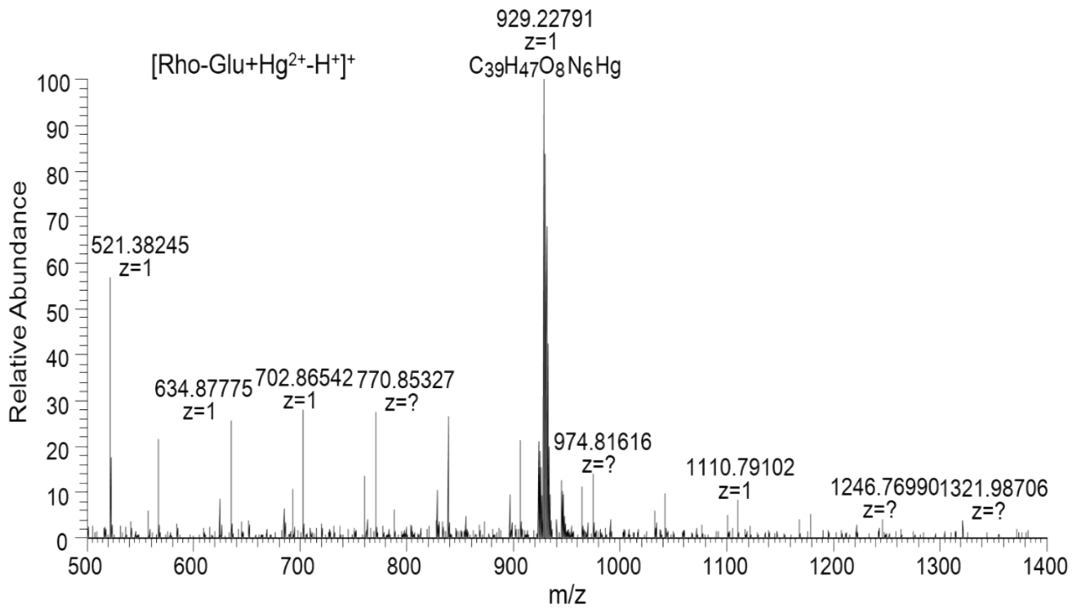


**Fig. S15** Mass spectrum of Rho-Glu-$Hg^{2+}$ complex

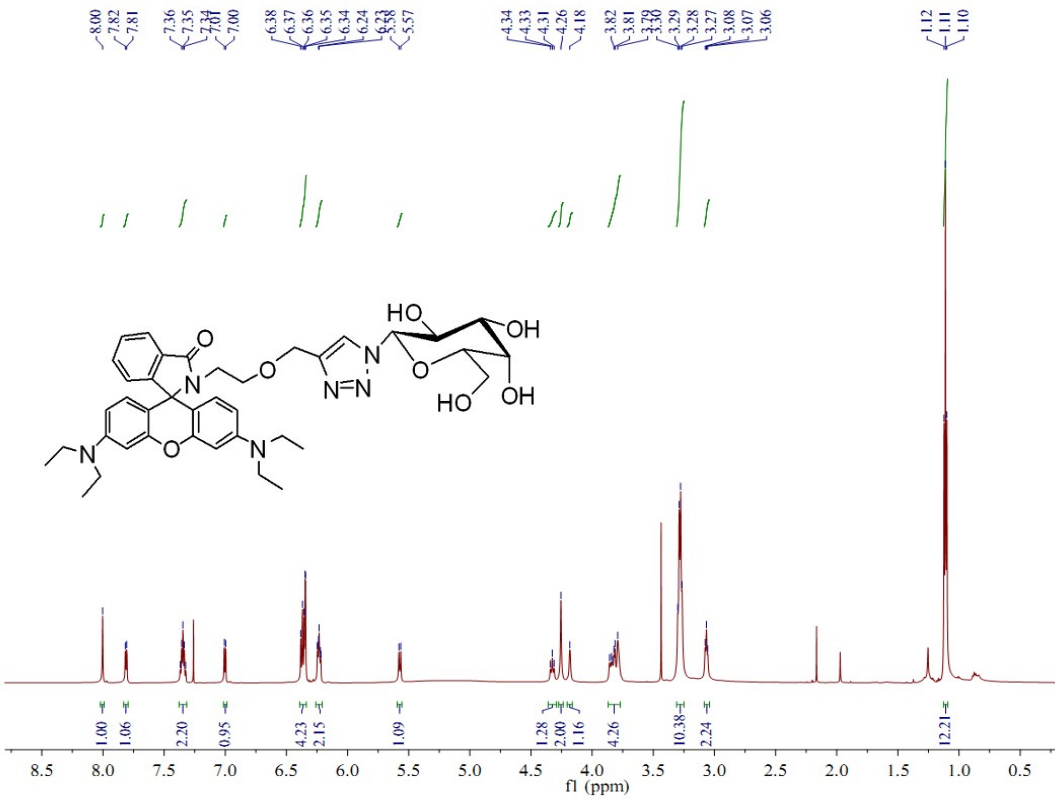


**Fig. S16** $^{1}$H NMR of Rho-Gal

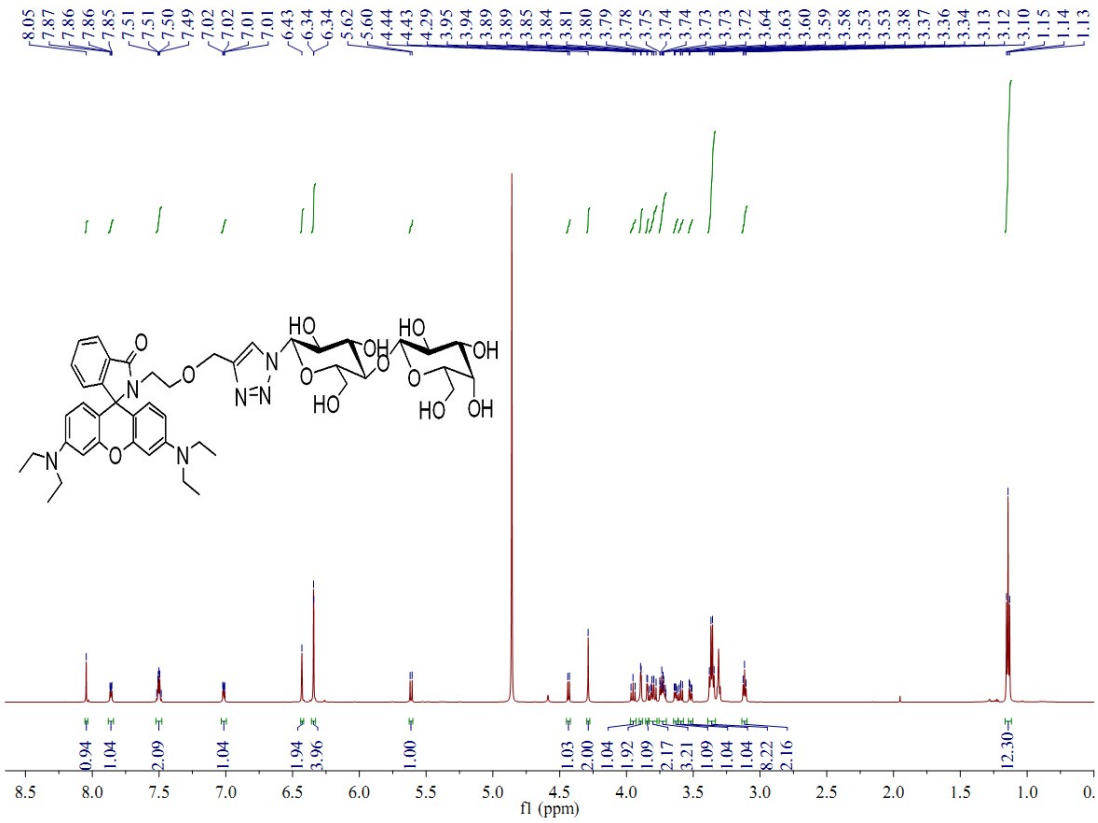


**Fig. S17** $^{1}$H NMR of Rho-Lac

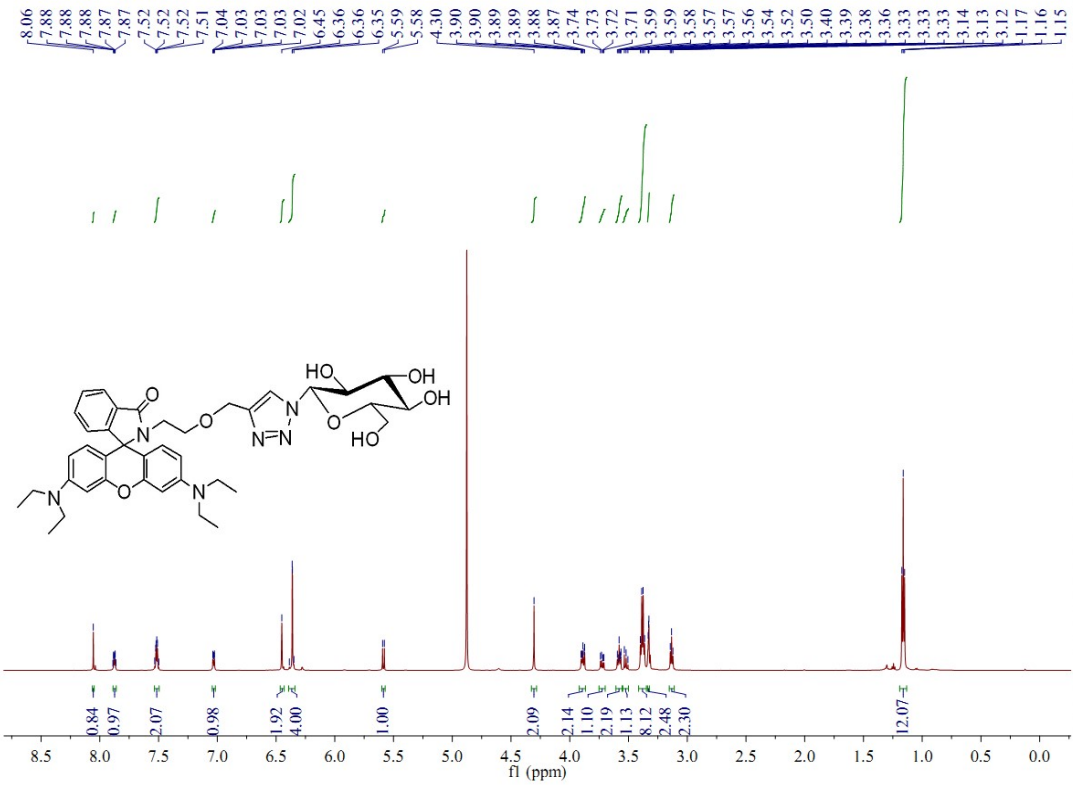


**Fig. S18** $^{1}$H NMR of Rho-Glu

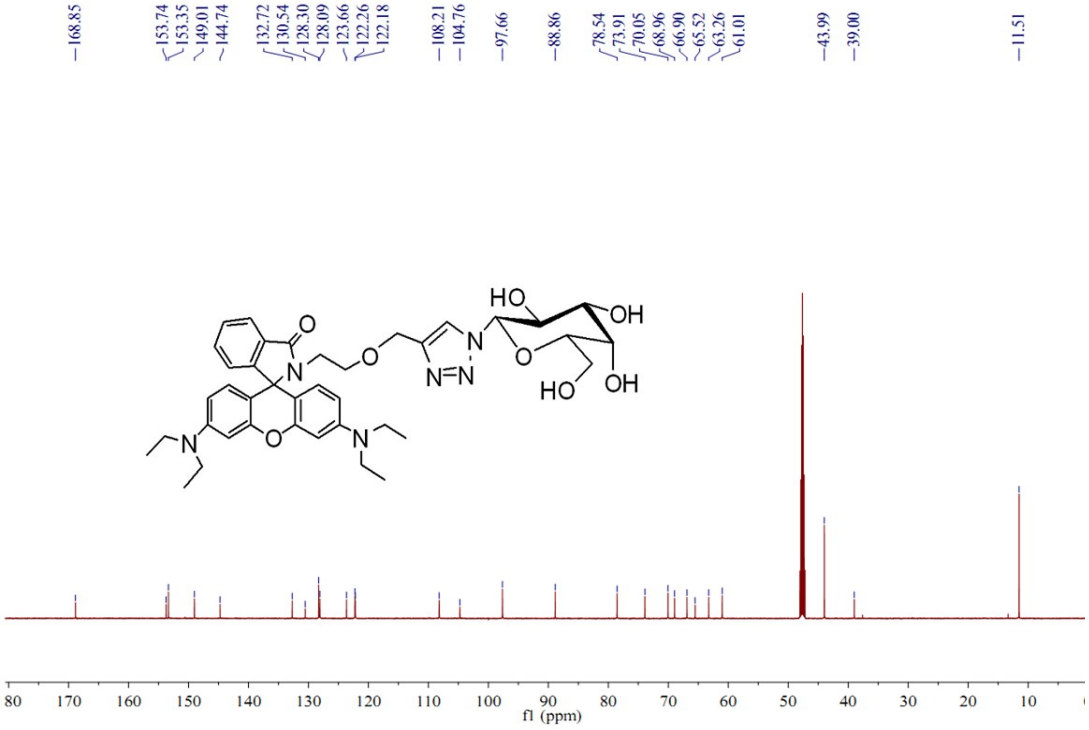


**Fig. S19** $^{13}$C NMR of Rho-Gal

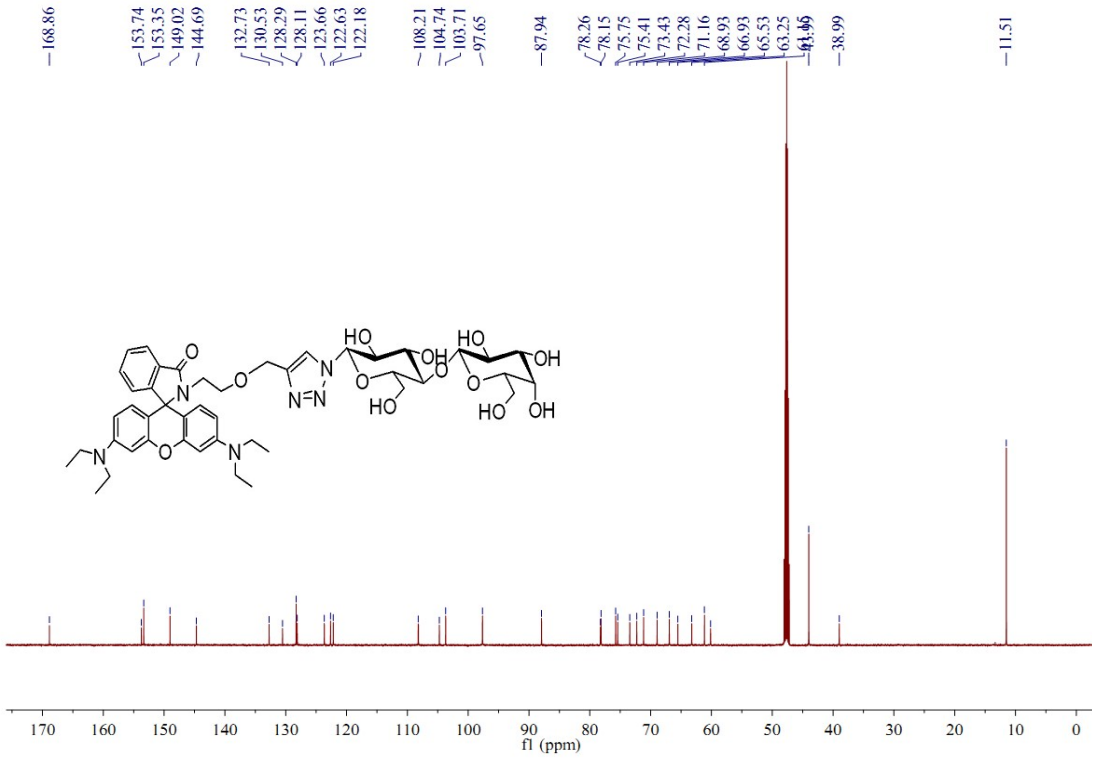


**Fig. S20** $^{13}$C NMR of Rho-Lac

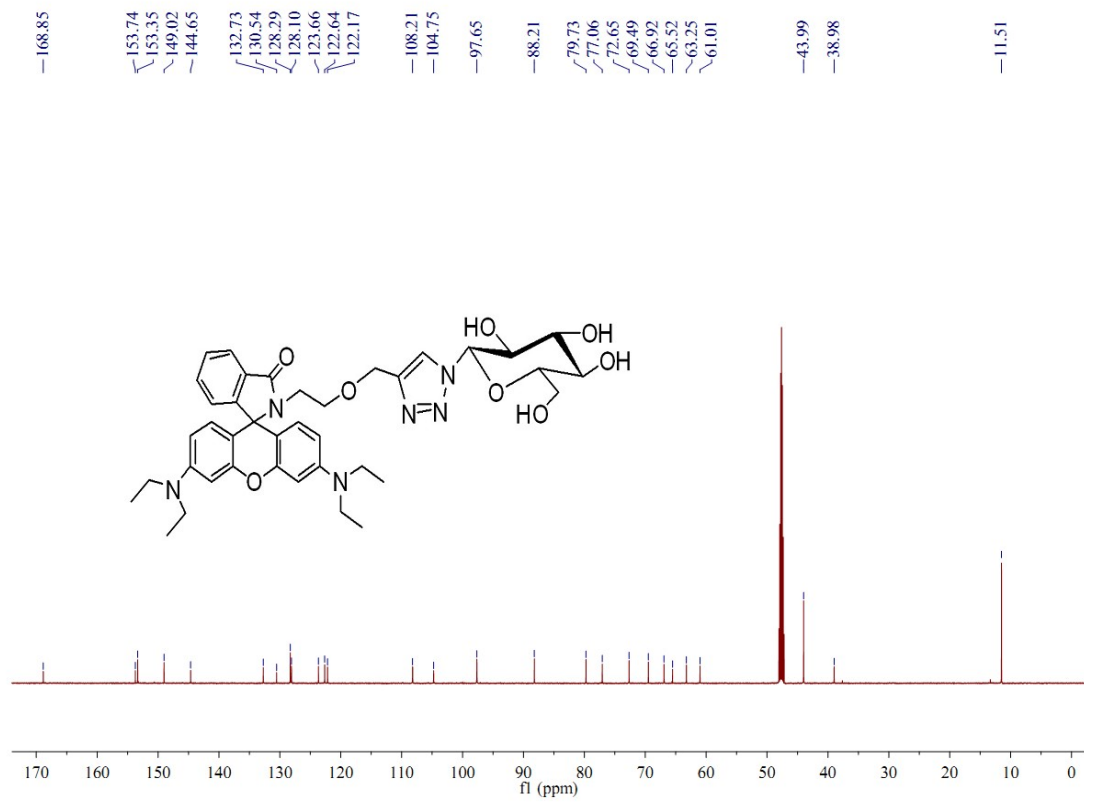


**Fig. S21** $^{13}$C NMR of Rho-Glu